Supplemental Materials for Biased Backpressure Routing Using Link Features and Graph Neural Networks

Zhongyuan Zhao, *Member, IEEE,* Bojan Radojičić, Gunjan Verma, Ananthram Swami, *Life Fellow, IEEE,* and Santiago Segarra, *Senior Member, IEEE*

I. Introduction

This technical report provides additional test results and list of notations to further supplement the main paper [3], which, though, is considered as self-contained.

II. Routes Visualization

Figs. 1(d) and 1(c) respectively show the routes for the exemplary flow exhibited in Fig. 1(a) under the SP-BP schemes SP-$\bar{r}/(xr)$ and SP-$1/(x)$, with everything else identical. Figs. 1(b), 1(d), and 1(c) show that SP-BP schemes do not rely on a single shortest path, exhibiting the flexibility of BP schemes in path finding. Compared to EDR-$\bar{r}$ with bias based on hop distance (Fig. 1(b)), the use of link duty cycle in SP-BP schemes reduces random walks and yields more concentrated routs, especially when link rates are also considered.

III. Additional test results for mixed traffic

This section provides additional test results for the mixed traffic setting in Section VII-B-3) of the main paper [3] with different node densities and/or interference levels. The outcomes of these tests are consistent with the test settings in the manuscript.

We first present the end-to-end latency performances of streaming and bursty traffics in Figs. 2(a) and 2(b), respectively, for wireless multihop networks generated from a node density of $12/\pi$ with everything else the same as the setting for Figs. 6 in the Section VII-B-3) of the main paper [3]. It can be observed that the latency is generally reduced compared to Figs. 5(a) and 5(b) in the paper [3], due to 50% increase in node density, and consequently higher connectivity density and shorter distance between nodes. However, the ranking of different routing schemes in Figures 2 is consistent with the main paper [3].

Z. Zhao and S. Segarra are with the Department of Electrical and Computer Engineering, Rice University, USA. e-mails: {zhongyuan.zhao, segarra}@rice.edu

B. Radojičić is with the Faculty of Technical Sciences, University of Novi Sad, Serbia. e-mail: bojanradojicic00@gmail.com. Work was done as a visiting scholar at Rice University.

G. Verma, and A. Swami are with the US Army's DEVCOM Army Research Laboratory, USA. e-mails: {gunjan.verma.civ, ananthram.swami.civ}@army.mil.

Research was sponsored by the Army Research Office and was accomplished under Cooperative Agreement Number W911NF-19-2-0269. The views and conclusions contained in this document are those of the authors and should not be interpreted as representing the official policies, either expressed or implied, of the Army Research Office or the U.S. Government. The U.S. Government is authorized to reproduce and distribute reprints for Government purposes notwithstanding any copyright notation herein.

Preliminary results were presented in [1], [2].

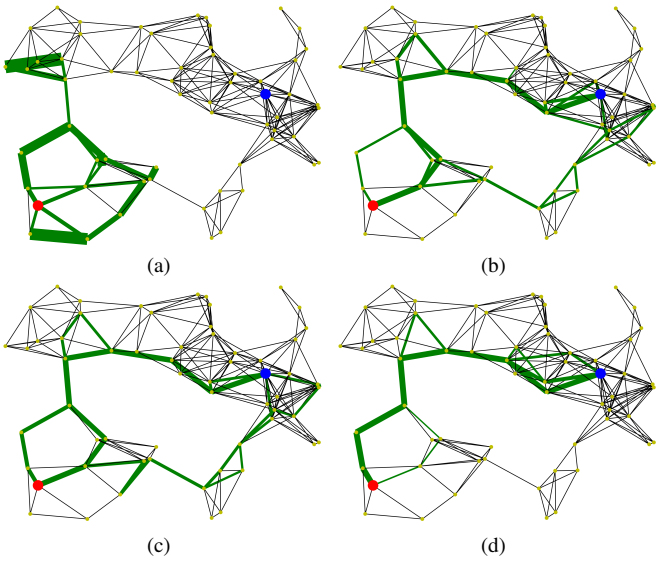

Fig. 1: Routes visualization for a flow from the red node to the blue node in a wireless multi-hop network with 60 nodes under multiple of BP schemes with everything else the same. The width of an edge is $1 + \sqrt[3]{n}$, where n is the number of packets sent over that link in 500 time steps; green edges indicate routes ($n > 0$). (a) Basic BP routing. (b) Enhanced dynamic BP routing (EDR) [4], [5] with a pre-defined bias given by a scaled shortest hop distance from a node to the destination. Our proposed SP-BP (c) SP-$1/x$ with link duty cycle, and (d) SP-$\bar{r}/(xr)$ with link rate and link duty cycle.

In Figs. 3(b) and 3(b), we respectively present the end-to-end latency performance of the streaming and bursty traffics with everything the same as Figs 2 but a lower interference level, captured by interface conflict model, i.e., two links are in conflict only if they share the same incidental node. Due to the lowered interference level, the network capacity is improved, and consequently, the latency is further reduced while the ranking of tested routing schemes remain consistent.

In Figs 4(a) and 4(b), we respectively present the end-to-end latency performance of the streaming and bursty traffics with everything the same as the manuscript except a lower interference level, captured by the interface conflict model. A lower interference level leads to reduced latency, while the ranking of the tested schemes are consistent with the Figs. 6(a) and 6(b).

We further compare the performance of GCNN and MLP under the proposed enhancements for SP-BP under two different interference levels: interface conflict model in Fig. 5(a) and unit-disk interference model in Fig. 5(b). The MLP is

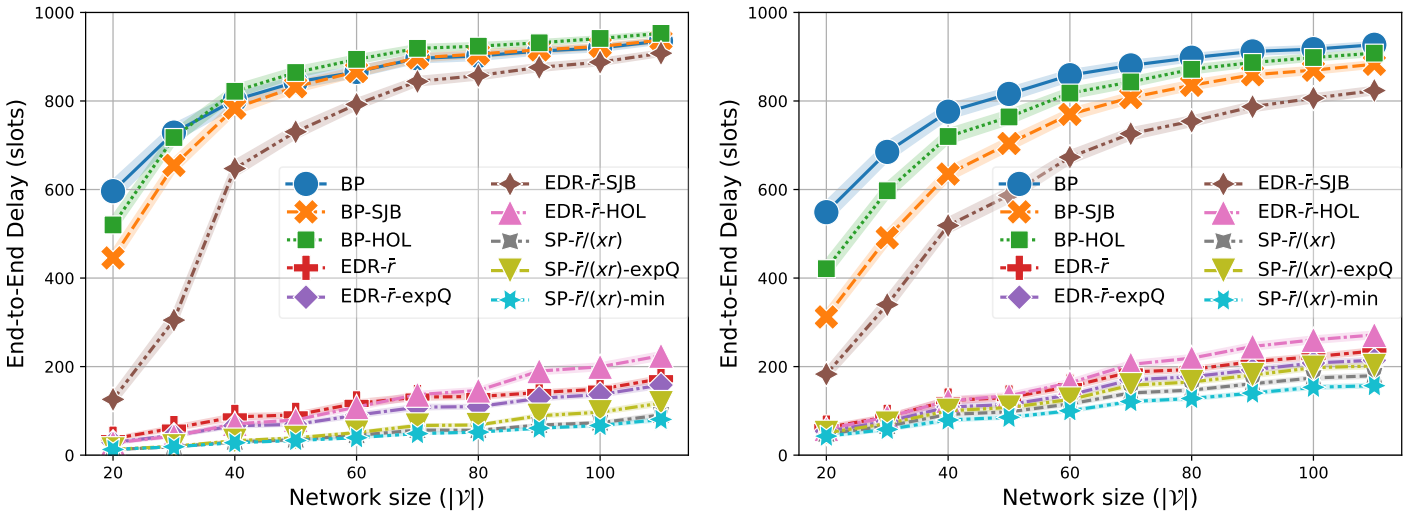

(a) Streaming traffics

(b) Bursty traffics

Fig. 2: End-to-end delay performance of streaming and bursty traffics in a mixed traffic configuration under networks generated from a higher node density of $12/\pi$ ($8/\pi$ in original manuscript), and unit-disk interference model.

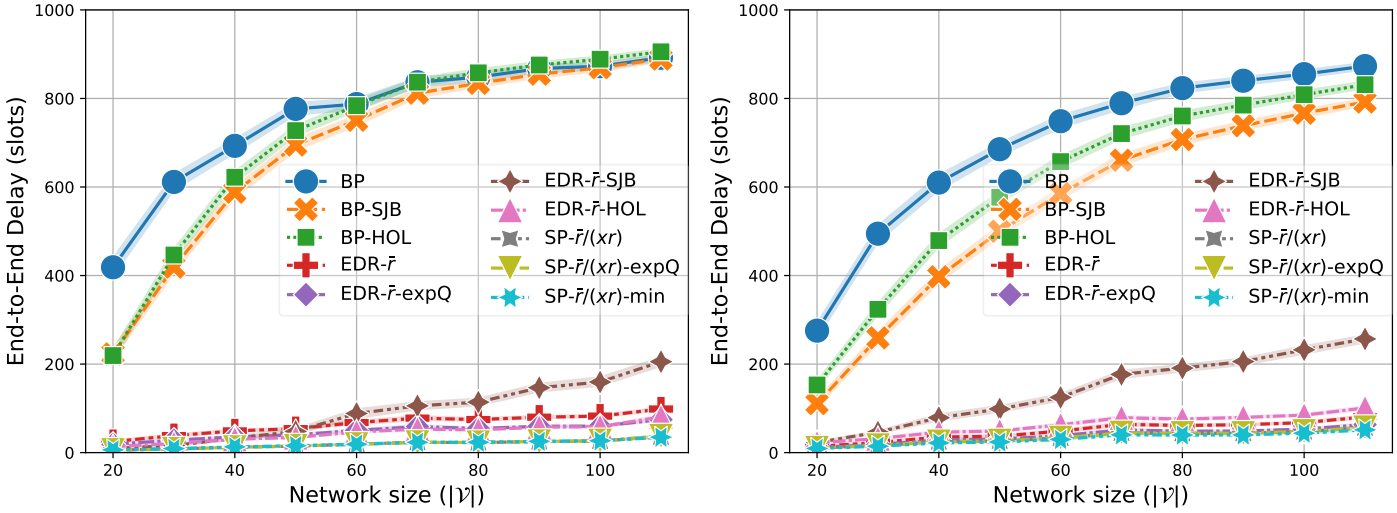

(a) Streaming traffics

(b) Bursty traffics

Fig. 3: End-to-end delay performance of streaming and bursty traffics in a mixed traffic configuration under networks generated from a higher node density of $12/\pi$ ($8/\pi$ in original manuscript), and interface conflict model.

configured with 5 dense layers with all the hidden dimensions of 32 and leaky ReLU activation in hidden layers, input feature as the conflict degree of each link (the node degree of conflict graph), and predicts its link duty cycle. The MLP is trained and tested in the same way as GCNN.

Although MLP doesn't require communications among nodes, it falls short in two aspects: 1) MLP underperforms GCNN even after optimal bias scaling is applied, showing that GCNN is better in encoding network topology into link duty cycle. 2) In the absence of optimal bias scaling, MLP fails to improve the latency compared to the baseline of EDR-$\bar{r}$, showing that MLP generalizes poorly under varying node density and interference level in terms of the scale of its output.

IV. List of Major Notations

Although all the notations in the main manuscript [3] have been described when they are referred for the first time, we list the major notations again in Table I along with their descriptions for readers to lookup.

References

[1] Z. Zhao, B. Radojicic, G. Verma, A. Swami, and S. Segarra, "Delay-aware backpressure routing using graph neural networks," in *IEEE Int. Conf. on Acoustics, Speech and Signal Process. (ICASSP)*, pp. 4720–4724, 2023.

[2] Z. Zhao, G. Verma, A. Swami, and S. Segarra, "Enhanced backpressure routing using wireless link features," in *IEEE Intl. Wrksp. Computat. Advances Multi-Sensor Adaptive Process. (CAMSAP)*, pp. 1–5, Dec. 2023.

[3] Z. Zhao, B. Radojičić, G. Verma, A. Swami, and S. Segarra, "Latency-improved backpressure routing using link features and graph neural networks," *IEEE Trans. Machine Learning in Commun. and Netw.*, 2024. submitted to.

[4] M. J. Neely, E. Modiano, and C. E. Rohrs, "Dynamic power allocation and routing for time-varying wireless networks," *IEEE J. Sel. Areas Commun.*, vol. 23, no. 1, pp. 89–103, 2005.

[5] L. Georgiadis, M. J. Neely, and L. Tassiulas, "Resource allocation and cross-layer control in wireless networks," *Foundations and Trends® in Networking*, vol. 1, no. 1, pp. 1–144, 2006.

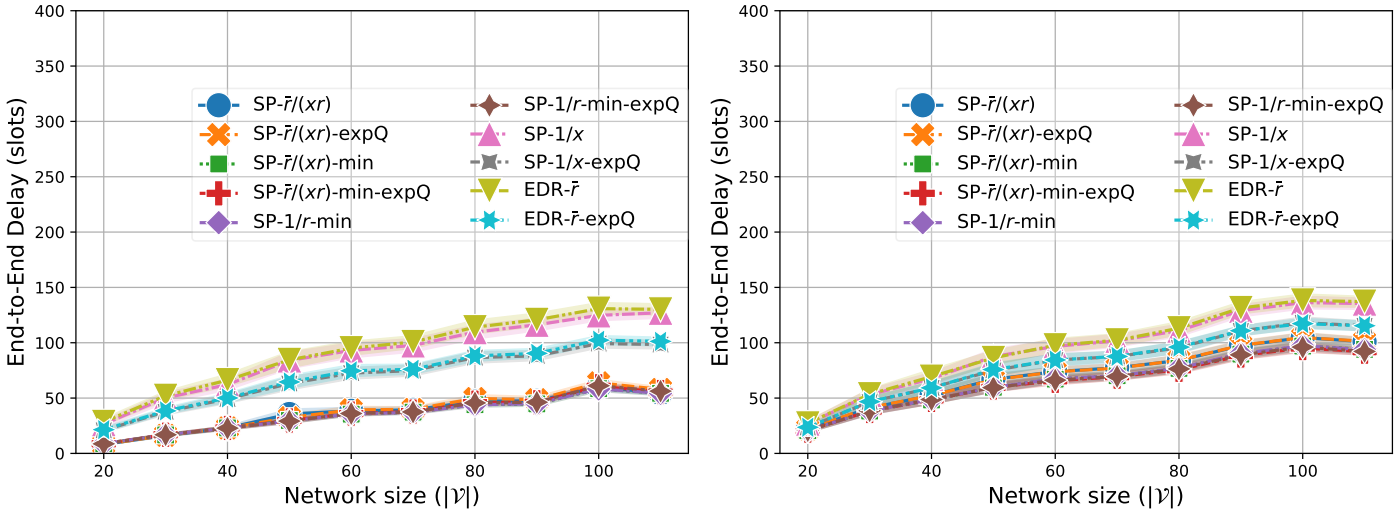

(a) Streaming traffics

(b) Bursty traffics

Fig. 4: End-to-end delay performance of streaming and bursty traffics in a mixed traffic configuration under networks generated from a node density of $8/\pi$ same as manuscript, but with lower interference level (interface conflict model).

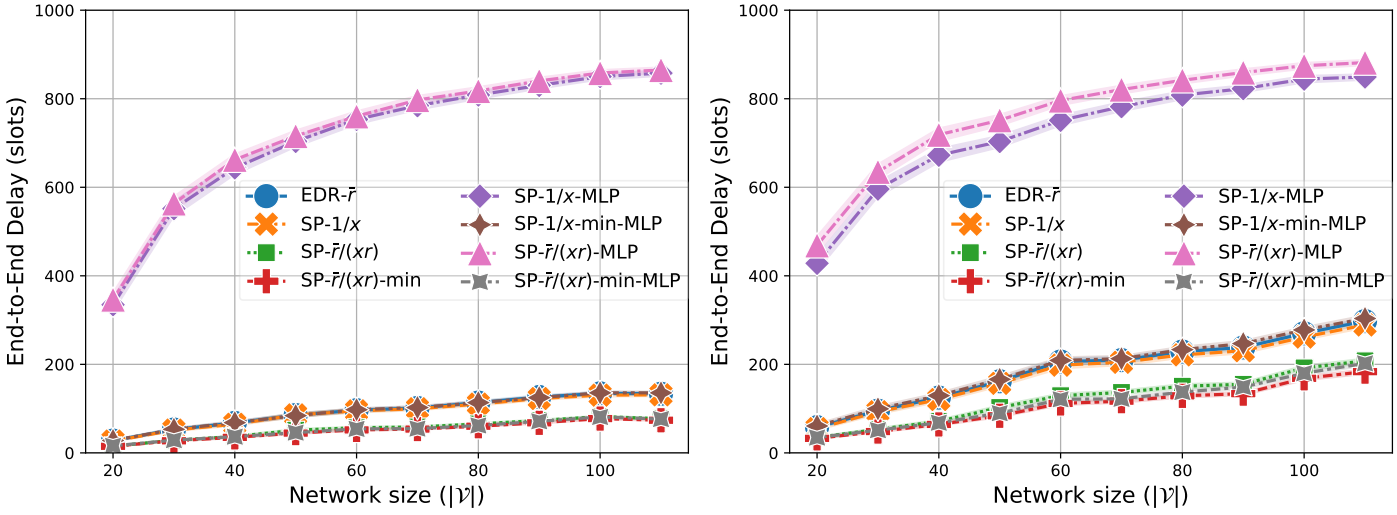

(a) Interface conflict model

(b) Unit-disk interference model

Fig. 5: End-to-end delay performance comparison between GCNN and MLP in mixed traffic setting where bursty flows are configured as heavier traffic

TABLE I: Descriptions of Major Notations

Symbols	Descriptions
α	learning rate
β	a positive constant used in Section VI in [3]
γ	a postive constant used in Section VI in [3]
δ_e	weight of link e for computing shortest path
$\Delta(t)$	Lyapunov drift
ϵ	the compounding parameter for expQ
$\mathbf{\Theta}_0^l, \mathbf{\Theta}_1^l$	sets of trainable parameters for layer l of GCN in (**??**)
$\lambda, \lambda(f)$	λ: arrival rate, $\lambda(f)$: arrival rate of flow f
$\mu_{ij}^{(c)}(t)$ $\mathbf{M}(t)$	the number of packets of commodity c to be transmitted from node i to node j at time step t $\mathbf{M}(t) \in \mathbb{Z}^{2\|\mathcal{E}\|\times\|\mathcal{V}\|}$: matrix collecting all $\mu_{ij}^{(c)}(t)$
$\mathbf{\Pi}$	Feasible space of routing and scheduling decisions
$\sigma_l(\cdot)$	activation function of layer l of GCN
$\mathbf{\Psi}_{\mathcal{G}^c}(\cdot;\boldsymbol{\omega})$	parameterized function of GCN defined on conflict graph $\mathcal{G}^c$, with a set of trainable parameters $\boldsymbol{\omega}$
Ω	target distribution of routing instances
$A_i^{(c)}(t)$	number of exogenous packets of commodity c arriving at node i during time slot t
$\mathbf{A}$	tensor collecting $A_i^{(c)}(t)$ for all $i, c \in \mathcal{V}$ and $t \leq T$
$B_i^{(c)}$ $\mathbf{B}$	QSI-agnostic bias for commodity c on node i matrix collecting $B_i^{(c)}$ for all $i, c \in \mathcal{V}$
c $c_{ij}^*(t)$	a commodity or the destination node of packets the optimal commodity on link (i,j) at t
$\mathcal{C}$	the set of conflict relations among wireless links
$d(v)$	degree of vertex v
D	diameter of unweighted connectivity graph $\mathcal{G}^n$
$\mathcal{E}$	the set of wireless links among mobile devices
$e = (i,j)$	a bidirectional wireless link $e \in \mathcal{E}$ between nodes $i, j \in \mathcal{V}$
$(\overrightarrow{i,j})$	a directed link for transmission from node i to node j
$\mathbb{E}(\cdot), \mathbb{1}(\cdot)$	$\mathbb{E}(\cdot)$: expectation, $\mathbb{1}(\cdot)$: indicator function
f	a flow or source-destination pair $f \in \mathcal{F}$
f_w	a function for edge weight defined in Section IV-B in [3]
$\mathcal{F}$	the set of all flows (source-destination pairs)
g_l	dimension of output features of layer l of GCN
$g(\cdot)$	a function of queue state information (QSI)
$\mathcal{G}^c = (\mathcal{E}, \mathcal{C})$	conflict graph, comprises vertex set $\mathcal{E}$ & edge set $\mathcal{C}$
$\mathcal{G}^n = (\mathcal{V}, \mathcal{E})$	connectivity graph, comprises vertex set $\mathcal{V}$ & edge set $\mathcal{E}$
L l	the total number of layers of GCN $l \in \{0, \ldots, L\}$: the index of a layer
$\mathcal{L}$	normalized Laplacian matrix of graph $\mathcal{G}^c$
$M_{i-}^{(c)}(t)$ $M_{i+}^{(c)}(t)$	packets of commodity c transmitted by node i at time t packets of commodity c received by node i at time t
$\mathcal{N}_{\mathcal{G}}(v)$	the set of immediate neighbors of vertex v on graph $\mathcal{G}$
$\mathbb{N}(a,b)$	normal distribution with mean a & standard deviation b
$Q_i^{(c)}(t)$	length of the queue for commodity c on node i at time t
$\mathcal{Q}_i^{(c)}(t)$	the QSI for commodity c on node i at time t
r, r_e $\mathbf{r}$	r (r_e): long-term link rate (of link $e \in \mathcal{E}$), the vector of long-term link rates for all links $\mathcal{E}$
$\bar{r}$	network-wide average long-term link rate
$\mathbf{R}$	$\mathbf{R} \in \mathbb{R}^{\|\mathcal{E}\|\times T}$ matrix captures instantaneous link rates
$\mathbf{s}$	$\mathbf{s} \in \{0,1\}^{\|\mathcal{E}\|}$ link schedule at time t
$U_i^{(c)}(t)$	backlog metric for commodity c on node $i \in \mathcal{V}$ at time t
$\mathbb{U}(a,b)$	uniform distribution between a and b
$\mathcal{V}$	the set of mobile devices
$w_{ij}(t)$ $\mathbf{w}(t)$	maximum backpressure of link $(\overrightarrow{i,j})$ at time t vector of $w_{ij}(t)$ for all directed links
$\tilde{w}_{ij}(t)$ $\tilde{\mathbf{w}}(t)$	$\tilde{w}_{ij}(t) = \max\{w_{ij}(t), w_{ji}(t)\}$ vector of $\tilde{w}_{ij}(t)$ for all bidirectional links
x $\mathbf{x}$	link duty cycle vector collecting all x_e for $e \in \mathcal{E}$